Article

molecular systems biology

Muscle cell atrophy induced by miR-155-5p reveals molecular targets in skeletal muscle disorders

Letícia Lopes [1], Sarah Santiloni Cury [1], Diogo de Moraes [1], Jakeline Santos Oliveira [1], Grasieli de Oliveira [1], Otavio Cabral-Marques [2,3,4,5,6], Geysson Javier Fernandez [1,7], Mario Hiroyuki Hirata [3], Da-Zhi Wang [8], Maeli Dal-Pai-Silva [1], Robson Francisco Carvalho [1]*, Paula Paccielli Freire [1,2,3]*

Abstract: MicroRNAs are small regulatory molecules that control gene expression. An emerging property of muscle miRNAs is the cooperative regulation of transcriptional and epitranscriptional events controlling muscle phenotype. miR-155 has been related to muscular dystrophy and muscle cell atrophy. However, the function of miR-155 and its molecular targets in muscular dystrophies remain poorly understood. Through *in silico* and *in vitro* approaches we identify distinct transcriptional profile of muscle cell atrophy induced by miR-155-5p. The atrophic myotubes changed the expression of 359 genes (166 up-regulated and 193 down-regulated). We reanalyzed muscle transcriptomic data from dystrophin-deficient patients and detected overlap with gene expression patterns in miR-155-treated myotubes. Our analysis indicated that miR-155 regulates a set of transcripts, including Aldh1l, Nek2, Bub1b, Ramp3, Slc16a4, Plce1, Dync1i1, and Nr1h3. Enrichment analysis demonstrates 20 targets involved in metabolism, cell cycle regulation, muscle cell maintenance, and immune system. Moreover, digital cytometry confirmed a significant increase in M2 macrophages, indicating miR-155 effects on immune response in dystrophic muscles. We highlight a critical miR-155 associated with disease-related pathways in skeletal muscle disorders.

Keywords: miR-155; microRNA; non-coding RNAs; muscular dystrophies; DMD; RNA-sequencing

1. Introduction

The skeletal muscle is the largest protein reservoir in the body and exhibits high plasticity in response to processes regulating growth, regeneration, metabolism, and atrophy (Miyazaki & Esser, 2009; Rennie *et al*, 2004). Muscle atrophy is characterized by decreased protein content, muscle fiber diameter, force production, and increased fatigue (Glass, 2005; Jackman & Kandarian, 2004; Lecker *et al*, 2004). The ubiquitin-proteasome and autophagy-lysosome are the main cellular degradation systems that regulate muscle atrophy (Bodine *et al*, 2001; Zhao *et al*, 2007; Mammucari *et al*, 2008, 2007). Through protein degradation, these systems are also responsible for modulating cytokine expression, transcription, and epigenetic factors (Dogra *et al*, 2006; Muñoz□Cánoves *et al*, 2013; Dogra *et al*, 2007). Furthermore, cytokines and growth factors modify signaling pathways that promote protein assembly and organelle turnover (Dogra *et al*, 2006; Muñoz□Cánoves *et al*, 2013; Dogra *et al*, 2007). The complexity of the mechanisms that induce muscle atrophy is regulated by non-coding RNAs, including microRNAs (miRNAs).

miRNAs are small non-coding RNAs that control gene expression post-transcriptionally (Kozomara *et al*, 2019; Lau *et al*, 2001; Lee & Ambros, 2001; Pasquinelli *et al*, 2000; Filipowicz *et al*, 2008), leading to global effects on skeletal muscle fibers (Chen *et al*, 2006; Luo *et al*, 2013; McCarthy *et al*, 2009). It involves preferential targeting of mRNAs encoding transcription factors, kinases, and phosphatases, leading to amplified impacts (Hu *et al*, 2012). These miRNA-mediated effects orchestrate pathways and biological functions, broadening their spectrum of action in skeletal muscle function and diseases.

Among the diverse of miRNAs acting on skeletal muscles, miR-155 plays a crucial role in regulating the immune system, aging-related alterations, development, regeneration, and muscle wasting in cancer-associated cachexia (Eisenberg *et al*, 2007; Freire *et al*, 2017; Meyer *et al*, 2015; Nie *et al*, 2016; Parkes *et al*, 2015; Seok *et al*, 2011; Zhao *et al*, 2012; Liu *et al*, 2022). miR-155 influences myoblast proliferation and differentiation into myotubes during *in vitro* myogenesis (Freire *et al*, 2017; Seok *et al*, 2011) and is consistently increased in primary muscular disorders, such as Duchenne muscular dystrophy (DMD) (Eisenberg *et al*, 2007; Parkes *et al*, 2015). Under such conditions, Eisenberg *et al.* (Eisenberg *et al*, 2007) demonstrated that mRNA-miRNAs predicted interactions in DMD participate in muscle regeneration, suggesting a specific physiological pathway underlying disease pathology.

[1] Department of Structural and Functional Biology, Institute of Biosciences, São Paulo State University (UNESP), Botucatu, SP, Brazil; leticia.oliveira@unesp.br (L.L.); santiloni.cury@unesp.br (S.C.); dioxiide2@gmail.com (D.M.); jakeline.oliveira@unesp.br (J.O.); oliveira.grase@gmail.com (G.O.); maeli.dal-pai@unesp.br (M.D.P)

[2] Department of Immunology, Institute of Biomedical Sciences, University of São Paulo, São Paulo, SP, Brazil; otavio.cmarques@gmail.com (O.C.M.)

[3] Department of Clinical and Toxicological Analyses, School of Pharmaceutical Sciences, University of São Paulo, São Paulo, SP, Brazil. mhhirata@usp.br (M.H.H.)

[4] Network of Immunity in Infection, Malignancy, and Autoimmunity (NIIMA), Universal Scientific Education and Research Network (USERN), Sao Paulo, Brazil.

[5] Department of Medicine, Division of Molecular Medicine, University of São Paulo School of Medicine

[6] Laboratory of Medical Investigation 29, University of São Paulo School of Medicine

[7] College of Medicine, University of Antioquia, UdeA, Medellín, Colombia; papacriolla@gmail.com (G.F.)

[8] Center for Regenerative Medicine, University of South Florida, Health Heart Institute, Tampa, FL, United States of America; dazhiw@usf.edu (D-Z. W.)

* Correspondence: robson.carvalho@unesp.br (R.F.C) or freirepp2@gmail.com (P.P.F.); Tel.: +55 14 3880 0473 R.F.C. or +55 11 3091 7397 P.P.F.

Given the emerging cooperative property of molecular networks regulated by miRNA targets, identifying the global transcriptional modulation triggered by miR-155 can help us understand post-transcriptional mechanisms in muscle diseases. Here, we characterized the transcriptional profile of muscle cells in response to increased miR-155 expression to identify direct and indirect sets of genes involved in skeletal muscle atrophy. We used computational biology and *in vitro* approaches to identify potential transcripts regulated by miR-155. Our investigation involved the C2C12 muscle cells and skeletal muscle samples obtained from individuals with DMD.

2. Results

2.1 Relevance of miR-155 in different skeletal muscle conditions

We reviewed the literature and observed that the expression of miR-155 is altered in myopathies, muscular dystrophies, muscle regeneration, and embryonic development of skeletal muscles (Supplementary Table 1). In addition to alterations in miR-155 expression in nine primary skeletal muscle diseases (Eisenberg *et al*, 2007), we performed a meta-analysis of transcriptome data obtained from different experimental murine or human samples with altered expression of miR-155 in skeletal muscle or C2C12 cells. Ten studies were identified in four conditions related to aging, muscular dystrophies, physical exercise, and skeletal muscle atrophy models. We observed increased expression of this miRNA in a mouse model of atrophy induced by desmin deletion (knockout) (GSE34388) (Meyer & Lieber, 2012). Meanwhile, miR-155 showed a tendency to increase expression without statistical significance (p-value = 0.077) in Duchenne's muscular dystrophy (GSE1007) (Haslett *et al*, 2003). In addition, no difference in the expression of this miRNA was observed in other muscle dystrophy models (GSE5304, GSE1776, GSE12580) (Stevenson *et al*, 2005; Stillwell *et al*, 2009), aging (GSE 25941, GSE674, GSE362) (Raue *et al*, 2012; Welle *et al*, 2003, 2004) and exercise studies (GSE43760) (Poelkens *et al*, 2013) (Figure 1, Supplementary Table S2).

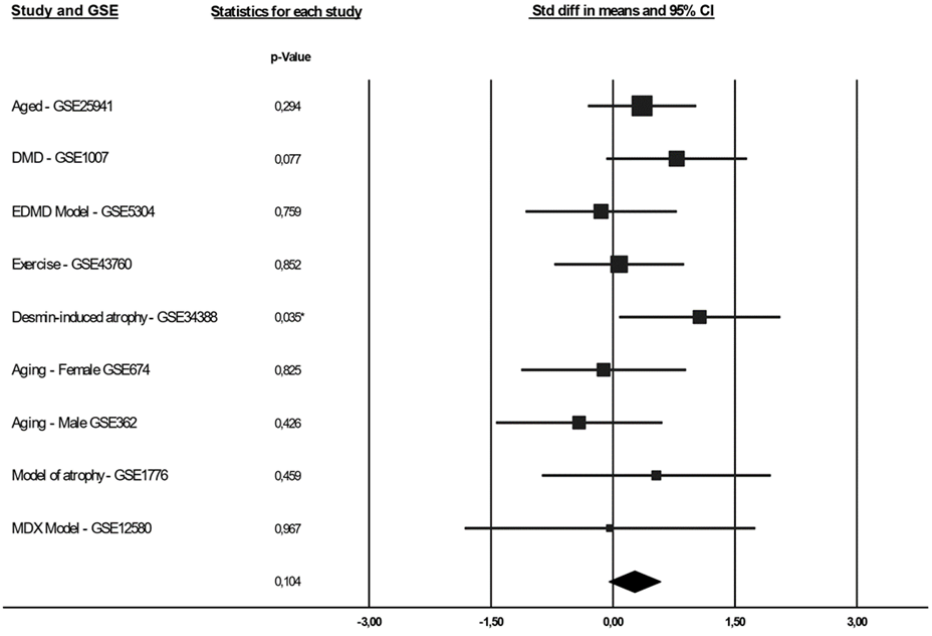

Figure 1. Forest plot (random-effects model) demonstrating alterations in the expression of the miR-155 in skeletal striated muscle under experimental conditions or animal models. Squares indicate a relative change in study-specific miR-155 (square size reflects study-specific statistical weight); horizontal lines indicate a 95% confidence interval (CI); and diamonds indicate the summary estimate of the relative change with a 95% CI.

2.2 miR-155 induces a transcriptional profile associated with morphological changes

To assess the potential changes in the myotube area induced by the increased expression of miR-155, we transfected C2C12 myotubes with mimic-miR-155-5p. This analysis revealed that miR-155 transfection significantly reduced the number and area of multinucleated myotubes (Figure 2A-B). Since it was previously demonstrated that miR-155 overexpression reduces myoblast proliferation and migration (Freire *et al*, 2017) , we next sought to evaluate the effects of mimic-miR-155 in both myoblast and myotube gene expression. Our transcriptome analysis using RNA-Seq of C2C12 cells transfected with miR-155 revealed 215 dysregulated transcripts in myoblasts (109 upregulated and 106 downregulated) and 359 in myotubes (165 upregulated and 194 downregulated) (Figure 2C-D, Supplementary Table S3).

We predicted the direct miR-155 targets using the miRWalk, miRTarBase, and TargetScan algorithms. We identified 511 transcripts predicted to be direct targets of miR-155. Among these direct targets, we identified five deregulated transcripts (*Cpm*, *Plce1*, *Dync1i1, Btc*, and *Nr1h3*) in the transcriptome of C2C12 myotubes transfected with miR-155 (Figure 2F). Additionally, miR-155 overexpression decreased the expression of *Ramp3* in both my-

oblasts and myotubes (Figure 2E). On the other hand, we found that miR-155 overexpression increased the expression of *Gm13454, Mybpc1, Gm16529*, and *Tmem262* in myoblasts and myotubes (Figure 2E).

To determine the intermediate regulators of miR-155 target transcripts (indirect targets), we assessed potential *in silico* transcription factors (TF) and kinases that regulate the set of differentially expressed genes induced by miR-155 overexpression in C2C12 myotubes. Our differentially expressed genes were indicated as controlled by a network of TF and kinases using the X2K web tool. These regulatory gene networks of TF and kinases were structured according to the molecule's connectivity, as indicated by network analysis using the Cytoscape program(Shannon *et al*, 2003) (Figure 3). For data representation, we used the four transcriptional factors with p-values < 0.05; and the top 10 kinases with p-values < 0.05, considering that 68 kinases were indicated as subnetwork regulators (Figure 3A, 3C). The transcription factors E2F4, SIN3A, and FOXM1 were suggested to regulate genes associated with phosphorylation during cell proliferation and differentiation, sarcomere rupture, and apoptosis (Figure 3B, 3D). MAPK14, CDK4, and HIPK2 were identified as kinases regulating genes associated with transcriptional activation and repression, cell cycle progression, inflammation, and fibrogenesis (Figure 3A, 3C).

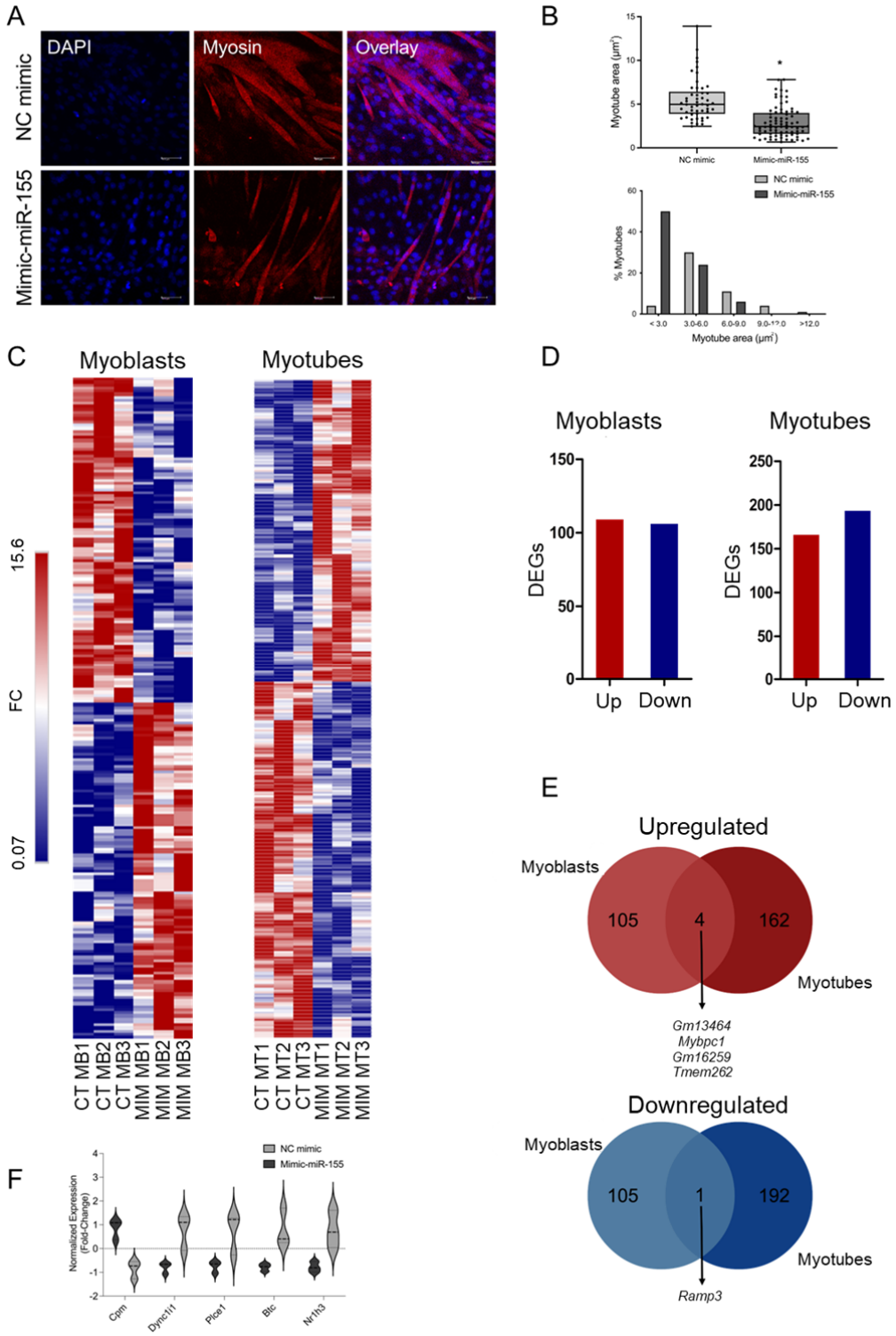

Figure 2. The gene expression profiles of C2C12 myoblasts and myotubes treated with miR-155 are distinct. FC (fold-change). (**A**) Immunofluorescence of C2C12 myotubes with mimic-miR-155 stained with an antibody that recognizes Myh2 (myosin heavy chain, red). DAPI-stained nuclei. (**B**) Quantitative analysis of C2C12 myotube size (top) and size distribution (bottom) in the control and miR-155-overexpressing cells. The myofiber area was determined using the ImageJ software. The data represent the mean ± standard deviation of at least three independent experiments. Statistical significance was analyzed using the Student's t-test. (**C**) Heatmap of differentially expressed genes (DEGs) between myoblast (MB) or myotube (MT) groups overexpressing miR-155 and their respective controls (CT; 1, 2, and 3 represent independent biological replicates for each group). Unsupervised hierarchical cluster analysis was performed using DEGs with p-value <0.05 and fold-change> 1.5 and is presented as a color scale. (**D**) Bar graphs show the number of DEGs (upregulated and downregulated) in miR-155-treated C2C12 myoblasts (left) and myotubes (right). (**E**) Venn diagram showing DEGs shared between miR-155-treated C2C12 myoblasts and myotubes. (**F**)

Normalized expression (RNA-Seq) of five potential direct targets of miR-155, identified by network analysis of C2C12 myotubes treated with miR-155 and their respective controls. P-value <0.05. NC mimic = control. Mimic-miR-155 = treatment.

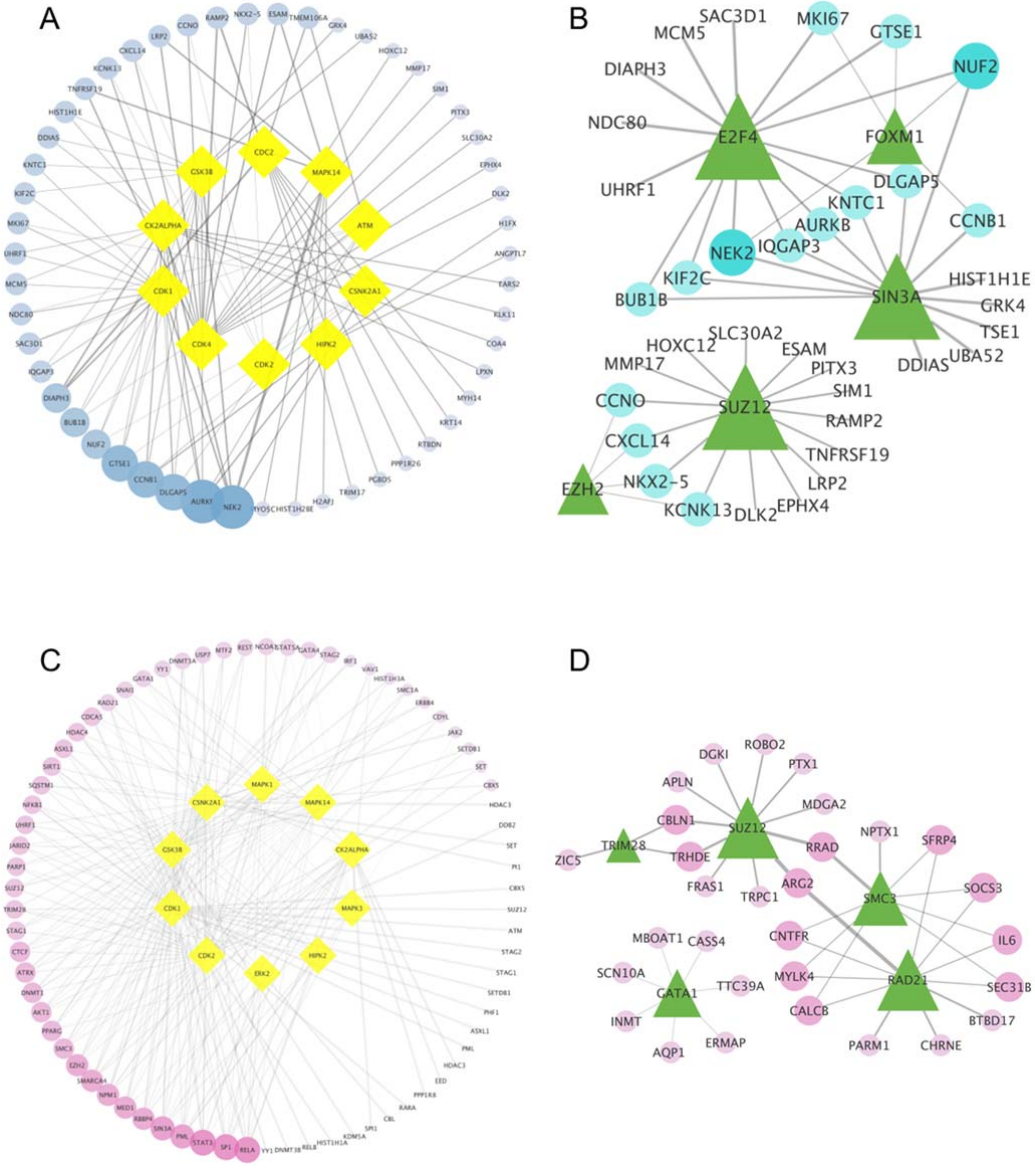

Figure 3. Potential transcription factors and kinases that regulate the DEGs of miR-155-treated C2C12 myotubes. Gene regulation network of differentially expressed genes (blue – down-regulated; pink – up-regulated), transcription factors (green triangles), and kinases (yellow diamonds), indicating gene enrichment. The genes (ellipse) and their regulatory kinases or transcription factors are sized based on the connectivity score (highest score → largest size). (A) Top 10 kinases (yellow) regulated by miR-155 that were down-regulated (blue). (B) Top five transcription factors (green) regulated by miR-155 that were down-regulated (blue). (C) Top 10 kinases (yellow) regulated by miR-155 that were up-regulated (pink). (D) Top 5 transcription factors (green) regulated by miR-155 that were up-regulated (pink).

2.3 Biological processes enriched in the transcriptome of miR-155-treated myoblasts and myotubes

We also investigated the biological processes enriched by DEG in myotubes and myoblasts treated with miRNA-155 (Figure 4). Overexpression of miR-155 induced specific transcriptional changes in C2C12 myoblasts and myotubes. The upregulated genes in miR-155-treated myoblasts were related to sarcomere organization, increased inflammatory responses, interleukin-6-mediated signaling pathways, and macrophage activation (Figure 4). In myotubes, genes with increased expression enriched cell cycle processes such as microtubule cytoskeleton organization involved in mitosis, complex-dependent catabolic process promoting anaphase, and nucleus division (Figure 4). Analysis of down-regulated genes in myoblasts identified different enriched categories associated with actin filament network formation, extracellular matrix assembly, cell-cell adhesion, and skeletal system development (Figure 4).

Furthermore, the down-regulated genes were enriched in functions related to protein tyrosine kinase activity, tube diameter regulation, and down-regulation of apoptotic cell removal in myotubes (Figure 4).

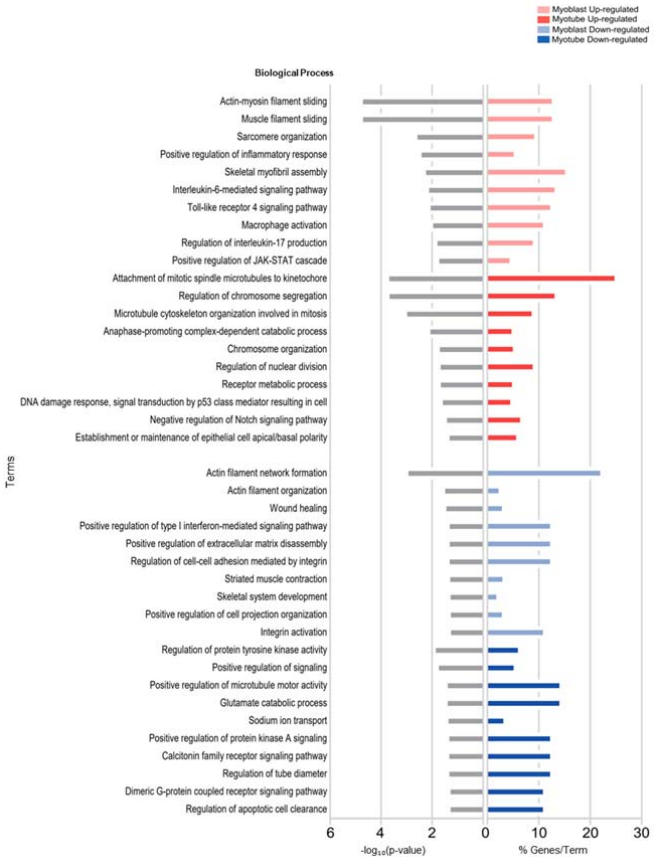

Figure 4. Biological processes enriched by miR-155-treated myoblasts and myotubes. C2C12 myotubes transfected with mimic-miR-155-5p induce gene expression changes associated with different functional categories. Gene ontology of differentially expressed genes (DEG) in C2C12 myoblasts after treatment with miR-155 to identify critical ontologies. Each horizontal bar on the left (gray bars) represents the number of enriched ontology terms presented in the dataset, considering -$\log_{10}$ (p-value). Each horizontal bar on the right (colored bars) represents the percentage of genes shown in the dataset compared with the total number of genes in each ontology. Fractions of DEGs in each lane (red, increasing; blue, decreasing) are shown on the x-axis.

2.4 The transcriptional overlap between miR-155 target and DMD patients

Through a study by Eisenberg *et al.* 2007 21, we sought to reanalyze the expression of miR-155 as one of the deregulated miRNAs in nine human muscle disorders. The selection criterion for the dataset was to search for homogeneous data between the number (n) of healthy controls and patients with muscle disorders. We retrieved a dataset of DMD samples (accession GSE1004) to investigate the differentially expressed genes in dystrophin-deficient patients and healthy skeletal muscles. We sought to identify a transcriptional profile overlapping the expression of miR-155-target genes in treated C2C12 myotubes with mimic-miR-155 and the transcriptome of muscle samples from DMD patients. Gene expression levels in DMD biopsies and normal skeletal muscle (GSE1004) were used for transcriptomic profile analysis. We compared our list of DEGs affected by the overexpression of the miR-155 with DEGs from 12 muscle biopsies with DMD (GSE1004). Overlap analysis identified 20 shared targets (Figure 5A). Among the direct targets of miR-155, we found three common genes downregulated in dystrophic samples: *Plce1, Dync1i1, and Nr1h3*, all exhibiting the same differential expression pattern. Of these 20 common targets, we focused on 18 genes that consistently appeared in our data analysis and previous literature (Supplementary Table S4-5) (Zhang *et al*, 2015, 2015; Ceafalan *et al*, 2015; Markert *et al*, 2008; Wirianto *et al*, 2020; Markert *et al*, 2010; Damal Villivalam *et al*, 2021; Hessvik *et al*, 2010; Zhang *et al*, 2016, 2018; Civatte *et al*, 2005; Baker *et al*, 2011; Wijshake *et al*, 2012; Okadome *et al*, 2018; Chen *et al*, 2018; Stuart *et al*, 2016; Zhu *et al*, 2016; Kelahmetoglu *et al*, 2020; Best *et al*, 2019; Lund *et al*, 2018; Hörbelt *et al*, 2019; Zhang *et al*, 2014; Cheung *et al*, 2011; Feng *et al*, 2017; Formigli *et al*, 2009; Gailly, 2012). Correlation analysis identified eighteen differentially expressed genes (Figure 5B). Enrichment analysis demonstrated that 20 shared target genes play a role in biological processes, such as metabolism, cell cycle, muscle cell maintenance, and the immune system. The Circos plot shows the four main categories of biological processes and their respective targets (Figure 5C). Interestingly, we observed that six genes (*Amhr2, Ccl3, Bub1b, Myh6, Slc16a4, and Trpc1)* are involved in immune responses. Furthermore, to

determine which type of immune cell would be the sensor for the immune response in DMD samples, we performed a CIBERSORT analysis that indicated a significant increase in M2 macrophages (Figure 5D-E).

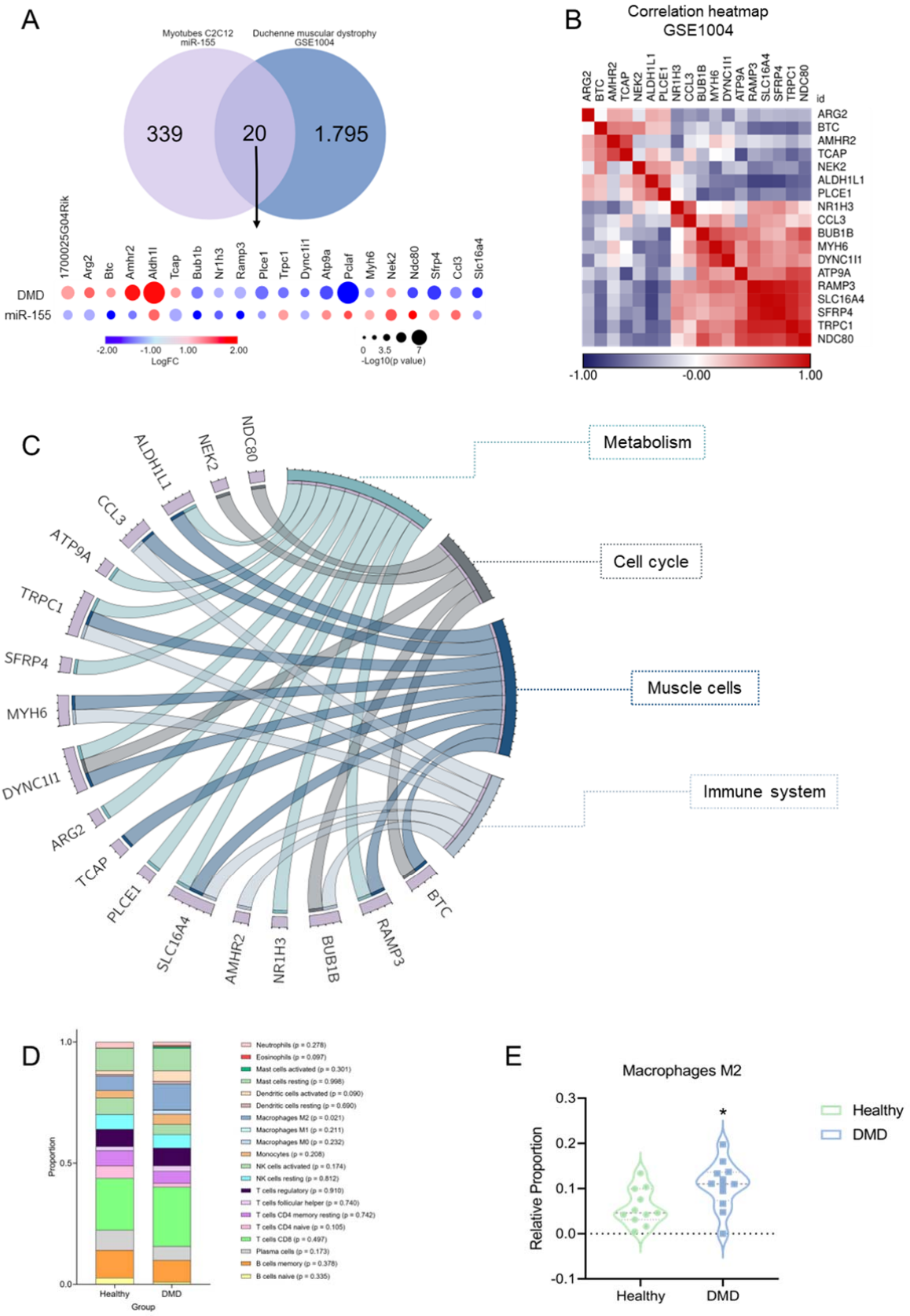

Figure 5. miR-155 mediates immunomodulatory pathology in Duchenne Muscular Dystrophy (DMD). (**A**) Comparative Bubble heatmap plotted in nodes to represent 20 differentially expressed genes in patients with DMD and C2C12 myotubes treated with miR-155. Consider the colors for $\log_{10}$FC (fold change) and dimensioned by -$\log_{10}$(p-value). (**B**) Correlation heatmap of gene expression data using microarrays (HG_U95Av2) of quadriceps biopsies from 12 DMD patients. Unsupervised hierarchical cluster analysis was performed using DEGs with p-value <0.05 and fold-change >1.5 and is presented as a color scale. The data are presented in Supplementary Table S4. (**C**) The circle represents the genes shared between the four biological categories (metabolism, cell cycle, muscle cells, and immune system). (**D**) The proportion of immune cells associated with differentially expressed genes was similar between patients with DMD and healthy controls. (**E**) The relative proportion of M2 macrophages in 12 muscle samples from DMD patients was statistically significantly compared with healthy control (p-value = 0.021).

2.5 Direct and indirect targets of miR-155-Based Network

Analysis of gene pathways under the post-transcriptional control of miR-155 revealed multiple gene interactions contributing to the cellular immune response (Figure 6A). These findings indicate that miR-155 plays a crucial role in regulating inflammatory processes in skeletal muscle under atrophic and dystrophic conditions. We observed that genes indirectly associated with the regulatory network are predominantly translated into kinases and transcription factors.

Specifically, *CSNK2A1*, which encodes CK2, a constitutively active protein kinase, was identified in this study (Götz & Montenarh, 2017; Meggio & Pinna, 2003; Salvi *et al*, 2009). Deletion of CK2β in myofibers results in a myasthenic phenotype, whereas CK2α'-null mice exhibit a reduced regeneration area in muscle fibers after injury (Cheusova *et al*, 2006; Shi *et al*, 2012). CK2 subunits are critical in regulating Myod1 expression and controlling myoblast fusion (Cheusova *et al*, 2006). Additionally, CK2 binds to the tyrosine kinase BUB1B, producing the BUBR1 protein (Baker *et al*, 2008). Appropriate centrosomal localization of BUB1B is paramount for precise chromosome segregation during mitosis and the preservation of genomic stability (Okadome *et al*, 2018) (Figure 6B). BUBR1 deficiency in skeletal muscle activates p14ARF, protecting against aging-related deterioration and senescence (Baker *et al*, 2008). BUBR1 is also involved in mitotic checkpoints and has angiogenic functions (Baker *et al*, 2008; Okadome *et al*, 2018). Furthermore, these two essential kinases are regulated by the transcription factor TRIM28, which regulates skeletal muscle size and function (Steinert *et al*, 2021). Notably, TRIM28 acts as an indirect target of miR-155, mediating two gene hubs involved in cell cycle processes and muscle cells, thus contributing to the overall dysregulation observed in dystrophic muscles 76. TRIM28 exhibits predominant nuclear localization within skeletal muscle cells, signifying its pivotal role as a crucial constituent in the assembly of regulatory complexes and modulation of specific transcription factors and kinases (Steinert *et al*, 2021) (Figure 6B).

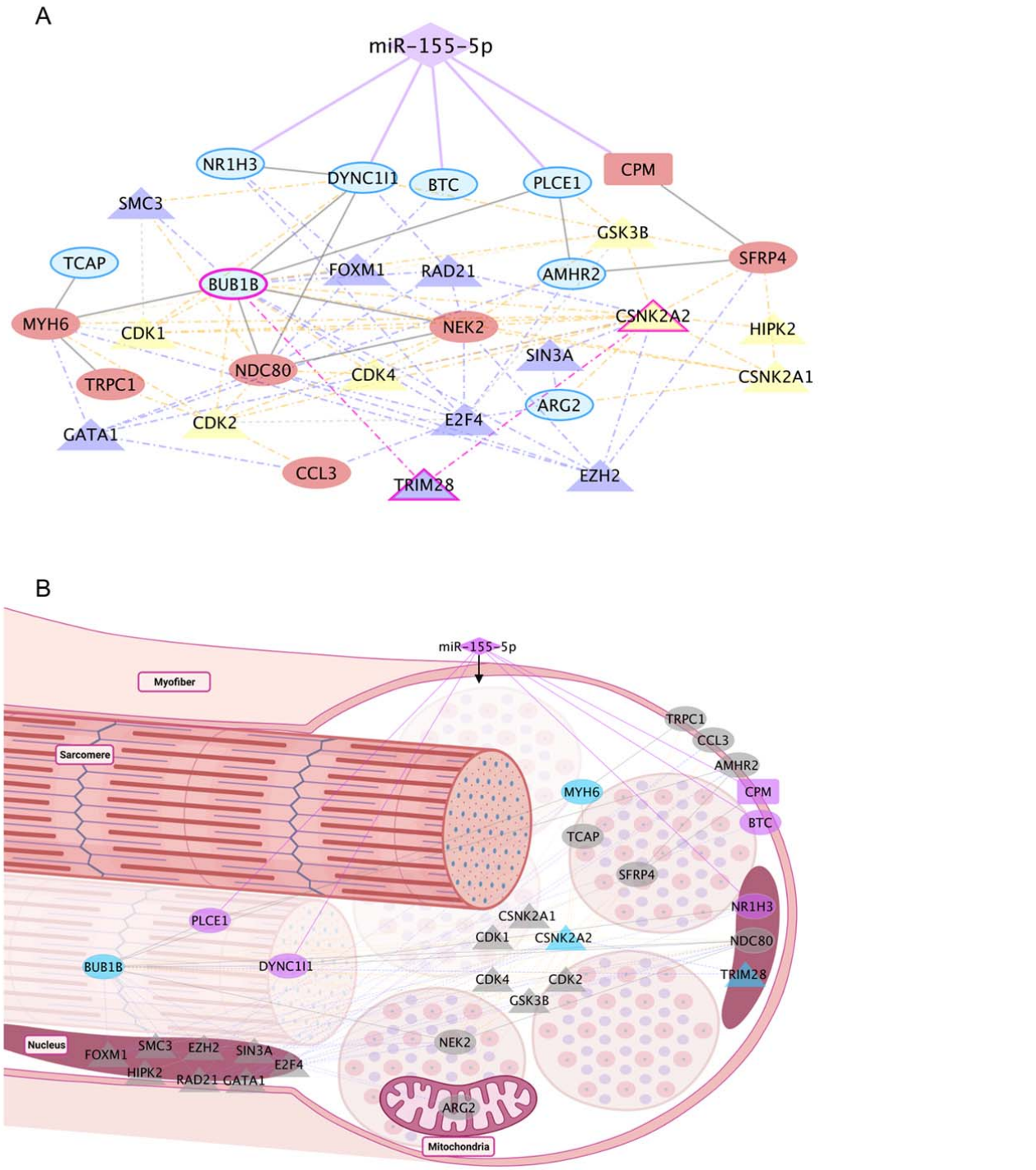

Figure 6. Integrated analysis revealed PPI pathways and regulatory factors associated with increased miR-155 expression in C2C12 skeletal muscle cells and individuals with DMD. The interaction network was predicted by the overlap of direct targets, TF, kinases, and common targets with DMD (GSE1004). (**A**) Gene regulatory network of differentially expressed genes induced by miR-155 overexpression. The five direct targets are linked to miR-155 by a solid purple line. Purple triangles represent transcription factors, and yellow triangles represent kinases. The genes described in blue show decreased expression in C2C12 cells treated with mimic-miR-155, and the genes shown in red show increased expression. Dashed lines represent indirect interactions caused by transcriptional factors or kinases. A solid gray line represents interactions between PPI. (**B**) The arrangement of the targets can be visualized in skeletal muscle cells. The TFs are purple, and the kinases are yellow. The solid purple line represents the direct interaction between miR-155-5p with the five direct targets. Purple nodes highlight the direct targets. Genes common to DMD are shown in ellipses. The rectangle highlights the gene *CPM* gene, which does not overlap with DMD. Diamond-shaped nodes represent TF and kinases. *BUB1B*, *CSNK2A2*, *TRIM28*, and *MYH6* are highlighted in blue as key targets (DMD and miR155).

3. Discussion

The present study aimed to identify direct and indirect targets of miR-155 in C2C12 skeletal muscle cells. Furthermore, integrating transcriptome data from individuals with DMD (public data) allowed us to establish crucial connections with our research objectives. Our results showed that miR-155 differently affected the gene expression profile of myoblasts and myotubes. The treatment of C2C12 myotubes with miR-155 regulated the expression of 359 genes mainly associated with inflammatory processes, dysregulation of the cell cycle, and apoptosis. Among these, 20 genes appeared to play pivotal roles in the muscle of DMD patients. Furthermore, the integrative analysis revealed that *Plce1, Dync1i1, Ramp3, Scl16a4, Nr1h3, and Bub1b* were downregulated in both miR-155-treated myotubes and skeletal muscle of dystrophic patients, whereas *Aldh1l and Nek2* were up-regulated. Thus, our results reveal a specific set of miR155-target genes potentially involved in the pathophysiology of DMD.

Several studies have demonstrated that miR-155 is a critical regulator of skeletal muscle plasticity (Freire *et al*, 2017; Nie *et al*, 2016; Seok *et al*, 2011; Curtale *et al*, 2019; O'Connell *et al*, 2007). Our morphometric analysis of myotubes transfected with miR-155 mimetic molecules agrees with these previous studies, demonstrating that miR-155 induces atrophy in C2C12 myotubes (Seok *et al*, 2011; Haslett *et al*, 2003). We observed that the overexpression of miR-155 significantly reduced the area and size of C2C12 myotubes. Our integrative analysis of different studies and data sets identified the relevance of miR-155 in various experimental and clinical conditions that affect skeletal muscles. In addition, when evaluating the transcriptome of C2C12 muscle cells transfected with miR-155, we noted that it mimicked an inflammatory and atrophic state (Figure 2A). Eisenberg *et al.*, 2007 (Eisenberg *et al*, 2007) investigated the expression profile of 185 miRNAs in 10 major muscle disorders in humans, including DMD. The authors observed that among the miRNAs analyzed, miR-155 was dysregulated in nine of these ten primary muscular dystrophies, suggesting the relevance of this miRNA in primary muscle disorders.

On the other hand, it is known that this miRNA plays an essential role in immune-mediated inflammatory myopathies. Macrophages also act as crucial regulators of the inflammatory response during skeletal muscle regeneration, affecting resident muscle cells, including myogenic and endothelial cells, and fibro-adipogenic progenitors involved in fibrofatty scar formation (Theret *et al*, 2022). While macrophage function is tightly coordinated during muscle regeneration, its dysregulation in muscular dystrophies leads to a chronic inflammatory state (Theret *et al*, 2022). Consistent with previous studies, our findings support the notion that dysregulation of miRNAs, including miR-155, occurs in response to inflammation associated with autoimmunity, potentially influencing muscle activation or degeneration processes and implicating muscle cell differentiation in macrophage-mediated inflammatory responses (Onodera *et al*, 2018; O'Connell *et al*, 2007; Georgantas *et al*, 2014). Furthermore, miR-155 in the immune response is essential for myeloid cell activation and balanced regulation of M1 and M2 macrophages during muscle regeneration (Nie *et al*, 2016). Our reanalysis of the study by Meyer and Lieber et al., 2012 (Meyer & Lieber, 2012), in which desmin was deleted in mice, resulted in skeletal muscle fibrosis and a significant increase in miR-155 expression. Moreover, infectious processes associated with pathogens and inflammatory stimuli, such as TNF or interferons, and even injury processes, lead to a rapid increase in the expression of miR-155 (Alivernini *et al*, 2018; Vigorito *et al*, 2013). Considering that fibrotic muscle adaptation without desmin increases the number of inflammatory cells, we note that myoblasts treated with mimic-miR-155 corroborate these investigations (Novak *et al*, 2017; Pillon *et al*, 2013). Although our findings and those of previous studies have demonstrated the pro-atrophic effects of this miRNA, the molecular mechanisms underlying its expression remain unknown.

Our transcriptome analysis indicated that miR-155 directly or indirectly controls genes that regulate biological functions in skeletal muscle diseases. Myoblasts and myotubes exhibited different gene expression patterns following miR-155 treatment. Quantitatively, myotubes had 144 additional DEGs compared with myoblasts. Regarding the direction of expression, only Receptor Activity Modifying Protein 3 (Ramp3) was downregulated in myoblasts and myotubes. In addition, only four transcripts were common when comparing upregulated genes in myoblasts and myotubes (*Gm13464*, *Mybpc1*, *Gm16259*, and *Tmem262*). Given the role of miRNAs as critical regulators of myogenesis, our observations revealed distinct gene expression profiles between myoblast and myotube stages, highlighting the enrichment of different gene sets (Figure 4). Specifically, in the myoblast stage, the enriched processes were primarily associated with differentiation and immune regulation, whereas in myotubes, the enriched processes were predominantly related to the cell cycle. Among the 359 dysregulated genes in C2C12 myotubes, five are potential direct targets of miR-155: *Cpm, Plce1, Dync1i1, Btc,* and *Nr1h3* (Figure 5A). Among these targets, *Cpm* showed an increase in expression in C2C12 myotubes with mimic-miR-155, which corroborates the findings of previous studies (Krause *et al*, 1998; Rehli *et al*, 2000; Tsakiris *et al*, 2012), linking this upregulation to inflammation, monocyte to macrophage differentiation, and M2-macrophage maturation (Krause *et al*, 1998; Rehli *et al*, 2000; Tsakiris *et al*, 2012). *Cpm* encodes a phosphoinositol-linked endopeptidase, an enzyme also associated with monocyte-macrophage differentiation in human cells of hematopoietic origin, suggesting an association between increased *Cpm* expression and cytotoxic macrophages (Krause *et al*, 1998). Additionally, this gene is involved in macrophage maturation, and its upregulation has been detected as a crucial selective marker for the differentiation of active lipid-laden macrophages, including the appearance of foam-cells *in vivo* (Krause *et al*, 1998; Rehli *et al*, 2000; Tsakiris *et al*, 2012). However, to our knowledge, no studies have shown the interaction between miR-155 and *Cpm* in conditions that induce skeletal muscle alterations. Among the direct targets that showed decreased expression after transfections with miR-155, *Btc* was involved in an angiogenic activity in trials with mice after acute mechanical trauma to the skeletal muscle (Ceafalan *et al*, 2015), an essential process during muscle regeneration. Another target, *Nr1h3* (or *Lxrα*), which plays a crucial role in macrophage response to intracellular bacterial infections (Joseph *et al*, 2004), inflammatory response, and metabolic homeostasis (A-González & Castrillo, 2011; Shavva *et al*, 2018), showed the same pattern of expression as observed in DMD samples. Although the ability of *Nr1h3* to regulate its

promoter induces the physiological response of macrophages to lipid loading, its expression in mouse cells or tissues is not similarly detectable. Still, the basis for this interspecies difference is unknown (A-González & Castrillo, 2011; Laffitte *et al*, 2001).

To understand how miR-155-affected genes might be involved in muscular dystrophies, we reanalyzed the transcriptome of DMD patients and found 20 overlapping genes with our data. Some of these genes play essential roles in immune response (Civatte *et al*, 2005; Zhang *et al*, 2018) (Supplementary Table S5). In myotubes, inhibiting the *Aldh1l1* transcription pathway restores oxidative stress and causes mitochondrial dysfunction (Damal Villivalam *et al*, 2021), *Tcap* knockdown inhibits the differentiation of myoblasts into myotubes (Markert *et al*, 2008; Wirianto *et al*, 2020), and its null mutation causes muscular limb-girdle dystrophy type 2G (LGMD2G) (Markert *et al*, 2010). *Bub1b* encodes a protein associated with mitotic checkpoint control (Baker *et al*, 2011), and *Ccl3* is a critical chemokine for idiopathic inflammatory myopathies, with high expression in injured skeletal muscle and responsible for recruiting Treg cells to these sites (Civatte *et al*, 2005; Zhang *et al*, 2018). Altogether, these data suggest that miR-155 and its targets *Plce1*, *Dync1i1*, *Ramp3*, *Scl16a4*, *Nr1h3*, *Bub1b*, *Aldh1l1,* and *Nek2* are involved in the pathological immune response of muscles in DMD patients, as indicated by the overlapping genes that control the inflammatory response. In this context, our reanalysis of DMD samples showed a higher proportion of M2 macrophages than in healthy human muscle tissues, and we reckoned that miR-155 can be delivered to muscle via M2 macrophages.

Moreover, the validation of the interaction with the set of genes must be performed in future studies to verify that miR-155 affects the phenotype of dystrophic cells. In addition, it is worth mentioning that the results showing an important change in the immune system corroborate studies of the top 18 genes shared between DMD and C2C12 myotubes with mimic-miR-155. Interactions with this set of genes should be validated in future studies to verify whether miR-155 affects the dystrophic cell phenotypes.

4. Materials and Methods

4.1 Literature review and meta-analysis

We performed a meta-analysis of studies data available in the literature (PubMed; https://www.ncbi.nlm.nih.gov/pubmed) that have identified changes in miR-155 expression in skeletal muscle or C2C12 cells under different experimental conditions. In addition, we searched the Entrez GEO Profiles database (https://www.ncbi.nlm.nih.gov/geoprofiles/) using the keywords "*miR-155 and skeletal muscle",* focusing on clinical studies and cell models (human and murine). We selected ten studies on different conditions, such as aging, muscular dystrophies, physical exercise, and models of skeletal muscle atrophy (Meyer & Lieber, 2012; Haslett *et al*, 2003; Stevenson *et al*, 2005; Stillwell *et al*, 2009; Raue *et al*, 2012; Welle *et al*, 2003, 2004; Poelkens *et al*, 2013). These selected studies showed alteration in the expression levels of miR-155 (p-value < 0.05; control vs. condition), according to the results of the GEO2R tool (https://www.ncbi.nlm.nih.gov/geo/geo2r/). The reanalyzed miR-155 expression data were presented in a forest plot generated by the Comprehensive Meta-Analysis software (https://www.metaanalysis.com/index.php?cart=BXVZ2967855).

4.2 Cell culture and muscle differentiation

C2C12 myoblast cells (ATCC® CRL-1772 TM) were cultured in Dulbecco's modified Eagle's Medium (DMEM, Thermo Fisher Scientific, USA) supplemented with 10% Fetal Bovine Serum (FBS, Thermo Fisher Scientific, USA), 1% penicillin-streptomycin (Thermo Fisher Scientific, USA) in a humidified incubator at 37 °C and 5% CO2. Subsequently, the cells were transferred to and cultured in 6-well plates (1×10^5 cells / well). C2C12 myoblasts were collected or induced to undergo myogenic differentiation after transfections with mimic-miR-155-5p. For differentiation, once the myoblasts reached 80-90% confluence, the growth medium was replaced with FBS-free, DMEM-containing Horse Serum (2%), L-glutamine, and penicillin/streptomycin (1%) for 120 h. All experiments were performed in triplicates for each group.

4.3 Oligonucleotides and transfection

The mimic-miR-155-5p (Thermo Fisher, mirVanaTM miRNA Mimic, code: 4464066; MC13058 - MC10203) and the respective negative control (CT) (Thermo Fisher, mirVanaTM miRNA Mimic Negative Control, code: 4464058) were transfected into C2C12 myoblasts, at 80% confluence. For transfection, the two complexes were combined into the final transfection solution. First, Lipofectamine RNAiMAX (Thermo Fisher, USA) was diluted in Opti-MEM® Reduced Serum Medium (Thermo Fisher, USA) to form the first complex. Next, mimic-miR-155 oligonucleotides and negative control were diluted in Opti-MEM® to form the second complex. Finally, Lipofectamine + Opti-MEM® complex was mixed with the oligonucleotide + Opti-MEM® complex and incubated for 5 min at room temperature. After this period, 250µl of the final transfection solution was added to each well containing C2C12 cells (80% confluent) in normal growth medium. The cells were then incubated for 15 h. Next, the myoblasts were transferred to a medium containing 2% horse serum to induce differentiation in myotubes. The myotube area and gene expression were analyzed after five days of differentiation. The experimental design for functional analysis of the miR-155-mimic during myogenesis is described in Supplementary Figure 1.

4.4 Immunostaining

For immunostaining, C2C12 myotubes treated in 6-well plates were fixed with 4% paraformaldehyde for 15 min, washed with PBS and 0.1% Triton X-100 (Sigma, USA), and incubated with a blocking solution containing 1% glycine, 3% BSA, 8% SFB in PBS and Triton X-100 for 1 h at room temperature. Primary antibody (Myh2) was incubated at 1: 600 dilution, then overnight at 4 °C and, washed with PBS, incubated with secondary antibody (anti-rabbit) at 1: 600 dilution for 2 h at 4 °C, and counterstained with DAPI (Vector Laboratories, USA). Digital fluorescent images were captured at room temperature using a TCS SP5 confocal scanning microscope (Leica Microsystems, UK). Myh2 pixels were counted using TCS SP5 (Leica Microsystems software, United Kingdom). ImageJ software measured the total nuclei, myotube nuclei, and myotube area. The fusion index was determined as (total myotube nucleus/total nucleus) x 100.

4.5 Total RNA extraction

Total RNA was extracted from C2C12 myotubes using TRIzol reagent (Thermo Fisher Scientific, USA), according to the manufacturer's instructions. Total RNA was quantified by spectrophotometry using a NanoVue spectrophotometer (GE Life Sciences, USA). The extracted RNA was treated with TURBO DNase (Thermo Fisher Scientific, USA) to remove contamination with genomic DNA. RNA quality was determined by RNA Integrity Number (RIN) using a 2100 Bioanalyzer system (Agilent, USA). Samples with RIN > 9 were considered in the subsequent analysis.

4.6 RNA sequencing

The construction of the RNA-Seq library for the CT (n = 3) and Mimic-mir-155 (n = 3) groups was based on 5 µg of total RNA according to the manufacturer's protocol using the Illumina HiScanSQ Instrument (Illumina, USA) and sequenced in the same flow cell as paired-end (2 × 100 bp). The sequencing generated an average of 25 million paired-end readings per sample. Raw sequence reads (.fastq files) were subjected to quality control analysis using the FastQC tool (version 0.11.5, http://www.bioinformatics.babraham.ac.uk/projects/fastqc/), and the process considered average quality scores Phred 20. For reading mapping of cDNA fragments, we used TopHat (version 1.3.2, http://tophat.cbcb.umd.edu) (Trapnell *et al*, 2012), a reading mapping algorithm capable of aligning RNA-Seq readings to a reference transcriptome in the case of the mouse (RefSeq, mm10). To count transcribed mapped readings and perform differential expression analysis, t R software HTSeq and DEseq packages (version 4.1.2, https://cran.r-project.org/bin/windows/base/), respectively, were used. We considered a fold-change >1.5 and a p-value <0.05.

4.7 Expression pattern visualization

The transcriptome data for C2C12 myoblast and myotube cells were represented by heatmaps generated using Morpheus software (https://software.broadinstitute.org/morpheus), which allows easy visualization and matrix analysis of the data sets. Venn's graphs, which showed the interaction of the myoblasts and myotubes DEGs, were generated from the Cacoo by Nulab 2019 software (https://cacoo.com/).

4.8 In silico prediction of direct target transcripts of miR-155

Potential miR-155 targets were predicted using the computational algorithms miRWalk (Sticht *et al*, 2018), miRTarBase (Huang *et al*, 2020), and TargetScan (Agarwal *et al*, 2015). Using more than one algorithm becomes essential to expand the number of predicted targets and filter the search by considering those mRNAs predicted by at least four distinct algorithms as possible targets. MiRWalk v.3.0 (http://mirwalk.umm.uni-heidelberg.de/) provides experimentally predicted and validated information (miRNA) about the miRNA-target interaction. This algorithm offers target miRNA predictions within the complete sequence for humans, rats, and mice. MiRTarBase v.7.0 (http://mirtarbase.mbc.nctu.edu.tw/php/search.php) has over 360.000 microRNA-Target interactions. The miRNA-target interactions collected are experimentally validated by reporter assays, western blotting, microarray, and sequencing experiments. TargetScan v.7.2 (http://www.targetscan.org/vert_72/) predicts miRNA biological targets by scanning for the presence of conserved 8mer, 7mer, and 6mer sites that correspond to regions essential for miRNA binding in the mRNA and uses curated updated miRNA families from Chiang et al., 2010 (Chiang *et al*, 2010) and Fromm et al., 2015 (Fromm *et al*, 2015).

4.9 In silico prediction of transcriptional factors and kinases

A network of transcriptional factors and kinases was predicted to regulate the differentially expressed genes of miR-155-treated myotubes, that is, the potential indirect targets, using the computational algorithms of the eXpression2Kinases (Clarke *et al*, 2018) (X2K Web; kinases, and transcriptional factors), and STRING Consortium v.11.0 (Szklarczyk *et al*, 2019) (protein-protein interaction). First, we considered transcriptional factors and kinases predicted by X2K Web (http://amp.pharm.mssm.edu/X2K/), with a p-value < 0.05. We then compared differentially expressed genes to the list of genes translated into mouse kinases and transcription factors to identify which presented altered expression. Finally, we connected these transcription factors and enriched kinases through known protein-protein interactions (PPIs) to build a subnetwork. The categories with a p-value < 0.05 were considered statistically significant.

4.10 Enrichment analysis

DEGs were used to identify enriched biological processes using the EnrichR tool (Chen *et al*, 2013; Kuleshov *et al*, 2016), powered by the Gene Ontology Consortium (Ashburner *et al*, 2000) (The Gene Ontology Consortium, 2019) (http://geneontology.org/) library 'GO_Biological_Process_2018', by PANTHER version 17.0 (Mi *et al*, 2021) (available at http://www.pantherdb.org/). Gene ontology (GO) categories with a p-value <0.05 were statistically significant. We use the REViGO (Supek *et al*, 2011) tool (http://revigo.irb.hr/) to summarize long lists of GO terms by removing redundant gene ontology terms. Ontology data were plotted using GraphPad Prism 8 software (https://www.graphpad.com/).

4.11 Differential expression analysis of dystrophin-deficient patients

We retrieved a data set of DMD samples (accession GSE1004) to investigate the differentially expressed genes in the skeletal muscles of dystrophin-deficient patients and healthy individuals. The dataset used in this analysis was selected from the GEO public repository maintained by the National Center for Biotechnology Information (NCBI) (https://www.ncbi.nlm.nih.gov/geo/) (Barrett *et al*, 2012). Intensity table was downloaded and processed, and DEGs between groups were identified using the Limma-Voom pipeline of the GEO2R web tool (https://www.ncbi.nlm.nih.gov/geo/geo2r/). Thus, the log transformation was automatically applied to the data using GEO2R. We applied the statistical cut-offs of log2 fold change > 1.2 and p-value < 0.05 to determine DEGs between DMD and normal samples. Next, we compared our list of 359 differentially expressed genes in miR-155-treated myotubes. The CIBERSORTx tool (https://cibersortx.stanford.edu/) was used to estimate cell fractions by relative proportion in the reanalysis of the two groups previously compared in GEO2R: 1) healthy skeletal muscle samples and 2) dystrophin-deficient patients (Aran *et al*, 2017). Gene expression normalized data with standard annotation was loaded into the CIBERSORTx algorithm, processed using the LM22 signature and 1000 permutations, and considered fractions with p-value < 0.05. Genes in major functional categories of the top genes shared between DMD samples, and C2C12 myotubes with mimic-miR-155 were displayed using the Circos plot (http://circos.ca/) (Krzywinski *et al*, 2009).

4.12 Reconstruction of molecular networks and data visualization

The direct targets of miR-155, in addition to its transcriptional factors (TF) and predicted kinases (see in "In silico prediction of transcriptional factors and kinases" section), were grouped by overlapping genes that were also deregulated in DMD samples. PPI networks were generated using the STRING Consortium v.11.0 (Szklarczyk *et al*, 2019). All interactions were derived from laboratory experiments with high-performance screening, text mining, and previous knowledge in selected databases with a high confidence level (sources: experiments, databases; confidence score ≥ 0.90). Furthermore, visualization and annotation of data from gene-PPI interaction networks were performed using the Cytoscape tool (Shannon *et al*, 2003). Finally, the graphical representation of the miR-targets inside the muscle cell was created with BioRender.com.

4.13 Statistical analysis

Values are reported as mean ± standard deviation (SD) unless otherwise indicated. Student's t-test was used to establish the DEGs (GraphPad Prism V.9) with significant values. P-values < 0.05 were considered statistically significant.

5. Conclusions

In conclusion, our findings indicate that miR-155 induces a distinct transcriptional profile of genes encoding proteins associated with anti-proliferative, pro-apoptotic, and inflammatory functions. Digital cytometry analysis of skeletal muscle samples from DMD patients revealed a potential association between miR-155 and M2 macrophages, suggesting its involvement in tissue remodeling and immune regulation. The increased expression of miR-155 leads to the downregulation of genes involved in apoptotic cell clearance, thereby compromising the efficiency of the apoptosis-signaling pathway. This observation highlights the gene expression pattern and regulatory directionality similarity between mimic-miR-155 and DMD. Furthermore, miR-155 directly controls the expression of at least five critical genes and indirectly influences numerous other genes through post-transcriptional processes. Our results support that miR-155 contributes to the atrophy of C2C12 muscle cells by orchestrating the regulation of genes involved in inflammation and apoptosis.

Supplementary Materials: Figure S1: Experimental design for the functional analysis of miR-155-mimic during myogenesis; Figure S2: Potential transcription factors and kinases that regulate the DEGs of miR-155-treated C2C12 myotubes; Table S1: Differentially Expressed Genes(DEGs) in C2C12 myotubes with mimic-miR-155; Table S2: Meta-analysis for a forest plot of conditions associated with skeletal muscle with altered miR-155 expression; Table S3: 18 Differently expressed genes in common between C2C12 muscle cells treated with miR-155 and Duchenne muscular dystrophy; Table S4: Role of important genes directly and indirectly deregulated by miR-155.

Author Contributions: L.L. wrote the manuscript and conducted the experimental analysis and the study. S.C., D.M., J.O., G.O., G.F., and O.C.M. conducted some analyses. G.F., L.L., R.F.C, and P.P.F conducted the RNA sequence analysis. M.H.H and D-Z.W. review the manuscript. R.F.C., M.D.P, and P.P.F. provided the infrastructure and intellectual content. R.F.C. and P.P.F

461 received funding, planned, and conducted the study, and wrote the manuscript. All authors have read and agreed to the published
462 version of the manuscript.

463 **Funding:** This research was funded by São Paulo Research Foundation (FAPESP), grant numbers #2018/23923-0,
464 #2020/01688-0, #2014/13783-6, #2020/09146-1, #13/50343-1, #12/13961-6.

465 **Data Availability Statement:** The RNAseq count table is available at GEO database number *GSEXXX - We are awaiting pub-*
466 *lication*. The DMD published microarray data can be found in the GEO database (GSE1004).

467 **Acknowledgments:** We acknowledge the São Paulo Research Foundation (FAPESP grants 2018/23923-0 to L.L.,
468 2020/01688-0 to O.C.M, 2014/13783-6 and 2020/09146-1 to P.P.F; 2013/50343-1 and 2012/13961-6 to R.F.C) for financial
469 support.

470 **Conflicts of Interest:** The authors declare no competing financial and/or non-financial interests in relation to the work described.

471 References

472 Agarwal V, Bell GW, Nam J-W & Bartel DP (2015) Predicting effective microRNA target sites in mammalian
473 mRNAs. *Elife* 4

474 A-González N & Castrillo A (2011) Liver X receptors as regulators of macrophage inflammatory and metabolic
475 pathways. *Biochim Biophys Acta* 1812: 982–994

476 Alivernini S, Gremese E, McSharry C, Tolusso B, Ferraccioli G, McInnes IB & Kurowska-Stolarska M (2018) Mi-
477 croRNA-155—at the Critical Interface of Innate and Adaptive Immunity in Arthritis. *Front Immunol* 8: 1932

478 Aran D, Hu Z & Butte AJ (2017) xCell: digitally portraying the tissue cellular heterogeneity landscape. *Genome Biol*
479 18: 220

480 Ashburner M, Ball CA, Blake JA, Botstein D, Butler H, Cherry JM, Davis AP, Dolinski K, Dwight SS, Eppig JT, *et al*
481 (2000) Gene ontology: tool for the unification of biology. The Gene Ontology Consortium. *Nat Genet* 25: 25–
482 29

483 Baker DJ, Perez-Terzic C, Jin F, Pitel KS, Pitel K, Niederländer NJ, Jeganathan K, Yamada S, Reyes S, Rowe L, *et al*
484 (2008) Opposing roles for p16Ink4a and p19Arf in senescence and ageing caused by BubR1 insufficiency. *Nat*
485 *Cell Biol* 10: 825–836

486 Baker DJ, Wijshake T, Tchkonia T, LeBrasseur NK, Childs BG, van de Sluis B, Kirkland JL & van Deursen JM (2011)
487 Clearance of p16Ink4a-positive senescent cells delays ageing-associated disorders. *Nature* 479: 232–236

488 Barrett T, Wilhite SE, Ledoux P, Evangelista C, Kim IF, Tomashevsky M, Marshall KA, Phillippy KH, Sherman PM,
489 Holko M, *et al* (2012) NCBI GEO: archive for functional genomics data sets—update. *Nucleic Acids Research*
490 41: D991–D995

491 Best JT, Xu P & Graham TR (2019) Phospholipid flippases in membrane remodeling and transport carrier biogene-
492 sis. *Curr Opin Cell Biol* 59: 8–15

493 Bodine SC, Latres E, Baumhueter S, Lai VK-M, Nunez L, Clarke BA, Poueymirou WT, Panaro FJ, Na E, Dharmara-
494 jan K, *et al* (2001) Identification of Ubiquitin Ligases Required for Skeletal Muscle Atrophy. *Science* 294: 1704–
495 1708

496 Ceafalan LC, Manole E, Tanase CP, Codrici E, Mihai S, Gonzalez A & Popescu BO (2015) Interstitial Outburst of
497 Angiogenic Factors During Skeletal Muscle Regeneration After Acute Mechanical Trauma. *Anat Rec (Hobo-*
498 *ken)* 298: 1864–1879

499 Chen EY, Tan CM, Kou Y, Duan Q, Wang Z, Meirelles GV, Clark NR & Ma'ayan A (2013) Enrichr: interactive and
500 collaborative HTML5 gene list enrichment analysis tool. *BMC Bioinformatics* 14: 128

501 Chen J-F, Mandel EM, Thomson JM, Wu Q, Callis TE, Hammond SM, Conlon FL & Wang D-Z (2006) The role of
502 microRNA-1 and microRNA-133 in skeletal muscle proliferation and differentiation. *Nat Genet* 38: 228–233

503 Chen R, Jiang T, She Y, Xie S, Zhou S, Li C, Ou J & Liu Y (2018) Comprehensive analysis of lncRNAs and mRNAs
504 with associated co-expression and ceRNA networks in C2C12 myoblasts and myotubes. *Gene* 647: 164–173

Cheung K-K, Yeung SS, Au SW, Lam LS, Dai Z-Q, Li Y-H & Yeung EW (2011) Expression and association of TRPC1 with TRPC3 during skeletal myogenesis. *Muscle Nerve* 44: 358–365

Cheusova T, Khan MA, Schubert SW, Gavin A-C, Buchou T, Jacob G, Sticht H, Allende J, Boldyreff B, Brenner HR, *et al* (2006) Casein kinase 2-dependent serine phosphorylation of MuSK regulates acetylcholine receptor aggregation at the neuromuscular junction. *Genes Dev* 20: 1800–1816

Chiang HR, Schoenfeld LW, Ruby JG, Auyeung VC, Spies N, Baek D, Johnston WK, Russ C, Luo S, Babiarz JE, *et al* (2010) Mammalian microRNAs: experimental evaluation of novel and previously annotated genes. *Genes Dev* 24: 992–1009

Civatte M, Bartoli C, Schleinitz N, Chetaille B, Pellissier JF & Figarella-Branger D (2005) Expression of the beta chemokines CCL3, CCL4, CCL5 and their receptors in idiopathic inflammatory myopathies. *Neuropathol Appl Neurobiol* 31: 70–79

Clarke DJB, Kuleshov MV, Schilder BM, Torre D, Duffy ME, Keenan AB, Lachmann A, Feldmann AS, Gundersen GW, Silverstein MC, *et al* (2018) eXpression2Kinases (X2K) Web: linking expression signatures to upstream cell signaling networks. *Nucleic Acids Res* 46: W171–W179

Curtale G, Rubino M & Locati M (2019) MicroRNAs as Molecular Switches in Macrophage Activation. *Front Immunol* 10: 799

Damal Villivalam S, Ebert SM, Lim HW, Kim J, You D, Jung BC, Palacios HH, Tcheau T, Adams CM & Kang S (2021) A necessary role of DNMT3A in endurance exercise by suppressing ALDH1L1-mediated oxidative stress. *EMBO J* 40: e106491

Dogra C, Changotra H, Mohan S & Kumar A (2006) Tumor Necrosis Factor-like Weak Inducer of Apoptosis Inhibits Skeletal Myogenesis through Sustained Activation of Nuclear Factor-κB and Degradation of MyoD Protein. *Journal of Biological Chemistry* 281: 10327–10336

Dogra C, Changoua H, Wedhas N, Qin X, Wergedal JE & Kumar A (2007) TNF-related weak inducer of apoptosis (TWEAK) is a potent skeletal muscle-wasting cytokine. *FASEB j* 21: 1857–1869

Eisenberg I, Eran A, Nishino I, Moggio M, Lamperti C, Amato AA, Lidov HG, Kang PB, North KN, Mitrani-Rosenbaum S, *et al* (2007) Distinctive patterns of microRNA expression in primary muscular disorders. *Proc Natl Acad Sci U S A* 104: 17016–17021

Feng L, Yang X, Asweto CO, Wu J, Zhang Y, Hu H, Shi Y, Duan J & Sun Z (2017) Genome-wide transcriptional analysis of cardiovascular-related genes and pathways induced by PM2.5 in human myocardial cells. *Environ Sci Pollut Res Int* 24: 11683–11693

Filipowicz W, Bhattacharyya SN & Sonenberg N (2008) Mechanisms of post-transcriptional regulation by microRNAs: are the answers in sight? *Nat Rev Genet* 9: 102–114

Formigli L, Sassoli C, Squecco R, Bini F, Martinesi M, Chellini F, Luciani G, Sbrana F, Zecchi-Orlandini S, Francini F, *et al* (2009) Regulation of transient receptor potential canonical channel 1 (TRPC1) by sphingosine 1-phosphate in C2C12 myoblasts and its relevance for a role of mechanotransduction in skeletal muscle differentiation. *J Cell Sci* 122: 1322–1333

Freire PP, Cury SS, de Oliveira G, Fernandez GJ, Moraes LN, da Silva Duran BO, Ferreira JH, Fuziwara CS, Kimura ET, Dal-Pai-Silva M, *et al* (2017) Osteoglycin inhibition by microRNA miR-155 impairs myogenesis. *PLoS One* 12: e0188464

Fromm B, Billipp T, Peck LE, Johansen M, Tarver JE, King BL, Newcomb JM, Sempere LF, Flatmark K, Hovig E, *et al* (2015) A Uniform System for the Annotation of Vertebrate microRNA Genes and the Evolution of the Human microRNAome. *Annu Rev Genet* 49: 213–242

Gailly P (2012) TRP channels in normal and dystrophic skeletal muscle. *Curr Opin Pharmacol* 12: 326–334

548 Georgantas RW, Streicher K, Greenberg SA, Greenlees LM, Zhu W, Brohawn PZ, Higgs BW, Czapiga M, More-
549 house CA, Amato A, *et al* (2014) Inhibition of myogenic microRNAs 1, 133, and 206 by inflammatory cyto-
550 kines links inflammation and muscle degeneration in adult inflammatory myopathies. *Arthritis Rheumatol* 66:
551 1022–1033
552 Glass DJ (2005) Skeletal muscle hypertrophy and atrophy signaling pathways. *Int J Biochem Cell Biol* 37: 1974–1984
553 Götz C & Montenarh M (2017) Protein kinase CK2 in development and differentiation. *Biomed Rep* 6: 127–133
554 Haslett JN, Sanoudou D, Kho AT, Han M, Bennett RR, Kohane IS, Beggs AH & Kunkel LM (2003) Gene expression
555 profiling of Duchenne muscular dystrophy skeletal muscle. *Neurogenetics* 4: 163–171
556 Hessvik NP, Boekschoten MV, Baltzersen MA, Kersten S, Xu X, Andersén H, Rustan AC & Thoresen GH (2010)
557 LXR{beta} is the dominant LXR subtype in skeletal muscle regulating lipogenesis and cholesterol efflux. *Am*
558 *J Physiol Endocrinol Metab* 298: E602-613
559 Hörbelt T, Knebel B, Fahlbusch P, Barbosa D, de Wiza DH, Van de Velde F, Van Nieuwenhove Y, Lapauw B,
560 Thoresen GH, Al-Hasani H, *et al* (2019) The adipokine sFRP4 induces insulin resistance and lipogenesis in
561 the liver. *Biochim Biophys Acta Mol Basis Dis* 1865: 2671–2684
562 Hu Y, Matkovich SJ, Hecker PA, Zhang Y, Edwards JR & Dorn GW (2012) Epitranscriptional orchestration of ge-
563 netic reprogramming is an emergent property of stress-regulated cardiac microRNAs. *Proc Natl Acad Sci U S*
564 *A* 109: 19864–19869
565 Huang H-Y, Lin Y-C-D, Li J, Huang K-Y, Shrestha S, Hong H-C, Tang Y, Chen Y-G, Jin C-N, Yu Y, *et al* (2020)
566 miRTarBase 2020: updates to the experimentally validated microRNA-target interaction database. *Nucleic*
567 *Acids Res* 48: D148–D154
568 Jackman RW & Kandarian SC (2004) The molecular basis of skeletal muscle atrophy. *Am J Physiol Cell Physiol* 287:
569 C834-843
570 Joseph SB, Bradley MN, Castrillo A, Bruhn KW, Mak PA, Pei L, Hogenesch J, O'connell RM, Cheng G, Saez E, *et al*
571 (2004) LXR-dependent gene expression is important for macrophage survival and the innate immune re-
572 sponse. *Cell* 119: 299–309
573 Kelahmetoglu Y, Jannig PR, Cervenka I, Koch LG, Britton SL, Zhou J, Wang H, Robinson MM, Nair KS & Ruas JL
574 (2020) Comparative Analysis of Skeletal Muscle Transcriptional Signatures Associated With Aerobic Exer-
575 cise Capacity or Response to Training in Humans and Rats. *Front Endocrinol (Lausanne)* 11: 591476
576 Kozomara A, Birgaoanu M & Griffiths-Jones S (2019) miRBase: from microRNA sequences to function. *Nucleic Ac-*
577 *ids Res* 47: D155–D162
578 Krause SW, Rehli M & Andreesen R (1998) Carboxypeptidase M as a marker of macrophage maturation. *Immunol*
579 *Rev* 161: 119–127
580 Krzywinski M, Schein J, Birol I, Connors J, Gascoyne R, Horsman D, Jones SJ & Marra MA (2009) Circos: an infor-
581 mation aesthetic for comparative genomics. *Genome Res* 19: 1639–1645
582 Kuleshov MV, Jones MR, Rouillard AD, Fernandez NF, Duan Q, Wang Z, Koplev S, Jenkins SL, Jagodnik KM,
583 Lachmann A, *et al* (2016) Enrichr: a comprehensive gene set enrichment analysis web server 2016 update.
584 *Nucleic Acids Res* 44: W90-97
585 Laffitte BA, Joseph SB, Walczak R, Pei L, Wilpitz DC, Collins JL & Tontonoz P (2001) Autoregulation of the Human
586 Liver X Receptor α Promoter. *Mol Cell Biol* 21: 7558–7568
587 Lau NC, Lim LP, Weinstein EG & Bartel DP (2001) An abundant class of tiny RNAs with probable regulatory roles
588 in Caenorhabditis elegans. *Science* 294: 858–862
589 Lecker SH, Jagoe RT, Gilbert A, Gomes M, Baracos V, Bailey J, Price SR, Mitch WE & Goldberg AL (2004) Multiple
590 types of skeletal muscle atrophy involve a common program of changes in gene expression. *FASEB J* 18: 39–
591 51

Lee RC & Ambros V (2001) An extensive class of small RNAs in Caenorhabditis elegans. *Science* 294: 862–864

Liu Y, Wang M, Deng T, Liu R, Ning T, Bai M, Ying G, Zhang H & Ba Y (2022) Exosomal miR-155 from gastric cancer induces cancer-associated cachexia by suppressing adipogenesis and promoting brown adipose differentiation via C/EPBβ. *Cancer Biol Med* 19: 1301–1314

Lund J, Aas V, Tingstad RH, Van Hees A & Nikolić N (2018) Utilization of lactic acid in human myotubes and interplay with glucose and fatty acid metabolism. *Sci Rep* 8: 9814

Luo W, Nie Q & Zhang X (2013) MicroRNAs Involved in Skeletal Muscle Differentiation. *Journal of Genetics and Genomics* 40: 107–116

Mammucari C, Milan G, Romanello V, Masiero E, Rudolf R, Del Piccolo P, Burden SJ, Di Lisi R, Sandri C, Zhao J, *et al* (2007) FoxO3 Controls Autophagy in Skeletal Muscle In Vivo. *Cell Metabolism* 6: 458–471

Mammucari C, Schiaffino S & Sandri M (2008) Downstream of Akt: FoxO3 and mTOR in the regulation of autophagy in skeletal muscle. *Autophagy* 4: 524–526

Markert CD, Meaney MP, Voelker KA, Grange RW, Dalley HW, Cann JK, Ahmed M, Bishwokarma B, Walker SJ, Yu SX, *et al* (2010) Functional muscle analysis of the Tcap knockout mouse. *Hum Mol Genet* 19: 2268–2283

Markert CD, Ning J, Staley JT, Heinzke L, Childers CK, Ferreira JA, Brown M, Stoker A, Okamura C & Childers MK (2008) TCAP knockdown by RNA interference inhibits myoblast differentiation in cultured skeletal muscle cells. *Neuromuscul Disord* 18: 413–422

McCarthy JJ, Esser KA, Peterson CA & Dupont-Versteegden EE (2009) Evidence of MyomiR network regulation of β-myosin heavy chain gene expression during skeletal muscle atrophy. *Physiological Genomics* 39: 219–226

Meggio F & Pinna LA (2003) One-thousand-and-one substrates of protein kinase CK2? *FASEB J* 17: 349–368

Meyer GA & Lieber RL (2012) Skeletal muscle fibrosis develops in response to desmin deletion. *Am J Physiol Cell Physiol* 302: C1609-1620

Meyer SU, Sass S, Mueller NS, Krebs S, Bauersachs S, Kaiser S, Blum H, Thirion C, Krause S, Theis FJ, *et al* (2015) Integrative Analysis of MicroRNA and mRNA Data Reveals an Orchestrated Function of MicroRNAs in Skeletal Myocyte Differentiation in Response to TNF-α or IGF1. *PLoS One* 10: e0135284

Mi H, Ebert D, Muruganujan A, Mills C, Albou L-P, Mushayamaha T & Thomas PD (2021) PANTHER version 16: a revised family classification, tree-based classification tool, enhancer regions and extensive API. *Nucleic Acids Research* 49: D394–D403

Miyazaki M & Esser KA (2009) Cellular mechanisms regulating protein synthesis and skeletal muscle hypertrophy in animals. *J Appl Physiol (1985)* 106: 1367–1373

Muñoz-Cánoves P, Scheele C, Pedersen BK & Serrano AL (2013) Interleukin-6 myokine signaling in skeletal muscle: a double-edged sword? *FEBS J* 280: 4131–4148

Nie M, Liu J, Yang Q, Seok HY, Hu X, Deng Z-L & Wang D-Z (2016) MicroRNA-155 facilitates skeletal muscle regeneration by balancing pro- and anti-inflammatory macrophages. *Cell Death Dis* 7: e2261

Novak JS, Hogarth MW, Boehler JF, Nearing M, Vila MC, Heredia R, Fiorillo AA, Zhang A, Hathout Y, Hoffman EP, *et al* (2017) Myoblasts and macrophages are required for therapeutic morpholino antisense oligonucleotide delivery to dystrophic muscle. *Nat Commun* 8: 941

O'Connell RM, Taganov KD, Boldin MP, Cheng G & Baltimore D (2007) MicroRNA-155 is induced during the macrophage inflammatory response. *Proc Natl Acad Sci U S A* 104: 1604–1609

Okadome J, Matsumoto T, Yoshiya K, Matsuda D, Tamada K, Onimaru M, Nakano K, Egashira K, Yonemitsu Y & Maehara Y (2018) BubR1 insufficiency impairs angiogenesis in aging and in experimental critical limb ischemic mice. *J Vasc Surg* 68: 576-586.e1

Onodera Y, Teramura T, Takehara T, Itokazu M, Mori T & Fukuda K (2018) Inflammation-associated miR-155 activates differentiation of muscular satellite cells. *PLoS ONE* 13: e0204860

636 Parkes JE, Day PJ, Chinoy H & Lamb JA (2015) The role of microRNAs in the idiopathic inflammatory myopathies.
637 *Curr Opin Rheumatol* 27: 608–615
638 Pasquinelli AE, Reinhart BJ, Slack F, Martindale MQ, Kuroda MI, Maller B, Hayward DC, Ball EE, Degnan B, Mül-
639 ler P, *et al* (2000) Conservation of the sequence and temporal expression of let-7 heterochronic regulatory
640 RNA. *Nature* 408: 86–89
641 Pillon NJ, Bilan PJ, Fink LN & Klip A (2013) Cross-talk between skeletal muscle and immune cells: muscle-derived
642 mediators and metabolic implications. *Am J Physiol Endocrinol Metab* 304: E453-465
643 Poelkens F, Lammers G, Pardoel EM, Tack CJ & Hopman MTE (2013) Upregulation of skeletal muscle inflamma-
644 tory genes links inflammation with insulin resistance in women with the metabolic syndrome. *Exp Physiol* 98:
645 1485–1494
646 Raue U, Trappe TA, Estrem ST, Qian H-R, Helvering LM, Smith RC & Trappe S (2012) Transcriptome signature of
647 resistance exercise adaptations: mixed muscle and fiber type specific profiles in young and old adults. *J Appl*
648 *Physiol (1985)* 112: 1625–1636
649 Rehli M, Krause SW & Andreesen R (2000) The membrane-bound ectopeptidase CPM as a marker of macrophage
650 maturation in vitro and in vivo. *Adv Exp Med Biol* 477: 205–216
651 Rennie MJ, Wackerhage H, Spangenburg EE & Booth FW (2004) Control of the size of the human muscle mass.
652 *Annu Rev Physiol* 66: 799–828
653 Salvi M, Sarno S, Cesaro L, Nakamura H & Pinna LA (2009) Extraordinary pleiotropy of protein kinase CK2 re-
654 vealed by weblogo phosphoproteome analysis. *Biochim Biophys Acta* 1793: 847–859
655 Seok HY, Tatsuguchi M, Callis TE, He A, Pu WT & Wang D-Z (2011) miR-155 inhibits expression of the MEF2A
656 protein to repress skeletal muscle differentiation. *J Biol Chem* 286: 35339–35346
657 Shannon P, Markiel A, Ozier O, Baliga NS, Wang JT, Ramage D, Amin N, Schwikowski B & Ideker T (2003) Cyto-
658 scape: a software environment for integrated models of biomolecular interaction networks. *Genome Res* 13:
659 2498–2504
660 Shavva VS, Mogilenko DA, Nekrasova EV, Trulioff AS, Kudriavtsev IV, Larionova EE, Babina AV, Dizhe EB,
661 Missyul BV & Orlov SV (2018) Tumor necrosis factor α stimulates endogenous apolipoprotein A-I expres-
662 sion and secretion by human monocytes and macrophages: role of MAP-kinases, NF-κB, and nuclear recep-
663 tors PPARα and LXRs. *Mol Cell Biochem* 448: 211–223
664 Shi X, Seldin DC & Garry DJ (2012) Foxk1 recruits the Sds3 complex and represses gene expression in myogenic
665 progenitors. *Biochem J* 446: 349–357
666 Steinert ND, Potts GK, Wilson GM, Klamen AM, Lin K-H, Hermanson JB, McNally RM, Coon JJ & Hornberger TA
667 (2021) Mapping of the contraction-induced phosphoproteome identifies TRIM28 as a significant regulator of
668 skeletal muscle size and function. *Cell Rep* 34: 108796
669 Stevenson EJ, Koncarevic A, Giresi PG, Jackman RW & Kandarian SC (2005) Transcriptional profile of a myotube
670 starvation model of atrophy. *J Appl Physiol (1985)* 98: 1396–1406
671 Sticht C, De La Torre C, Parveen A & Gretz N (2018) miRWalk: An online resource for prediction of microRNA
672 binding sites. *PLoS One* 13: e0206239
673 Stillwell E, Vitale J, Zhao Q, Beck A, Schneider J, Khadim F, Elson G, Altaf A, Yehia G, Dong J, *et al* (2009) Blasto-
674 cyst injection of wild type embryonic stem cells induces global corrections in mdx mice. *PLoS One* 4: e4759
675 Stuart CA, Stone WL, Howell MEA, Brannon MF, Hall HK, Gibson AL & Stone MH (2016) Myosin content of indi-
676 vidual human muscle fibers isolated by laser capture microdissection. *Am J Physiol Cell Physiol* 310: C381-389
677 Supek F, Bošnjak M, Škunca N & Šmuc T (2011) REVIGO summarizes and visualizes long lists of gene ontology
678 terms. *PLoS One* 6: e21800

679 Szklarczyk D, Gable AL, Lyon D, Junge A, Wyder S, Huerta-Cepas J, Simonovic M, Doncheva NT, Morris JH, Bork
680 P, *et al* (2019) STRING v11: protein-protein association networks with increased coverage, supporting func-
681 tional discovery in genome-wide experimental datasets. *Nucleic Acids Res* 47: D607–D613
682 Theret M, Saclier M, Messina G & Rossi FMV (2022) Macrophages in Skeletal Muscle Dystrophies, An Entangled
683 Partner. *J Neuromuscul Dis* 9: 1–23
684 Trapnell C, Roberts A, Goff L, Pertea G, Kim D, Kelley DR, Pimentel H, Salzberg SL, Rinn JL & Pachter L (2012)
685 Differential gene and transcript expression analysis of RNA-seq experiments with TopHat and Cufflinks.
686 *Nat Protoc* 7: 562–578
687 Tsakiris I, Torocsik D, Gyongyosi A, Dozsa A, Szatmari I, Szanto A, Soos G, Nemes Z, Igali L, Marton I, *et al* (2012)
688 Carboxypeptidase-M is regulated by lipids and CSFs in macrophages and dendritic cells and expressed se-
689 lectively in tissue granulomas and foam cells. *Lab Invest* 92: 345–361
690 Vigorito E, Kohlhaas S, Lu D & Leyland R (2013) miR-155: an ancient regulator of the immune system. *Immunol Rev*
691 253: 146–157
692 Welle S, Brooks AI, Delehanty JM, Needler N, Bhatt K, Shah B & Thornton CA (2004) Skeletal muscle gene expres-
693 sion profiles in 20-29 year old and 65-71 year old women. *Exp Gerontol* 39: 369–377
694 Welle S, Brooks AI, Delehanty JM, Needler N & Thornton CA (2003) Gene expression profile of aging in human
695 muscle. *Physiol Genomics* 14: 149–159
696 Wijshake T, Malureanu LA, Baker DJ, Jeganathan KB, van de Sluis B & van Deursen JM (2012) Reduced life- and
697 healthspan in mice carrying a mono-allelic BubR1 MVA mutation. *PLoS Genet* 8: e1003138
698 Wirianto M, Yang J, Kim E, Gao S, Paudel KR, Choi JM, Choe J, Gloston GF, Ademoji P, Parakramaweera R, *et al*
699 (2020) The GSK-3β-FBXL21 Axis Contributes to Circadian TCAP Degradation and Skeletal Muscle Function.
700 *Cell Rep* 32: 108140
701 Zhang B, Shang P, Qiangba Y, Xu A, Wang Z & Zhang H (2016) The association of NR1H3 gene with lipid deposi-
702 tion in the pig. *Lipids Health Dis* 15: 99
703 Zhang B-T, Yeung SS, Cheung K-K, Chai ZY & Yeung EW (2014) Adaptive responses of TRPC1 and TRPC3 during
704 skeletal muscle atrophy and regrowth. *Muscle Nerve* 49: 691–699
705 Zhang C, Qiao Y, Huang L, Li F, Zhang Z, Ping Y, Shen Z, Lian J, Li F, Zhao L, *et al* (2018) Regulatory T cells were
706 recruited by CCL3 to promote cryo-injured muscle repair. *Immunol Lett* 204: 29–37
707 Zhang J, Chen L, Long KR & Mu ZP (2015) Hypoxia-related gene expression in porcine skeletal muscle tissues at
708 different altitude. *Genet Mol Res* 14: 11587–11593
709 Zhao J, Brault JJ, Schild A, Cao P, Sandri M, Schiaffino S, Lecker SH & Goldberg AL (2007) FoxO3 Coordinately
710 Activates Protein Degradation by the Autophagic/Lysosomal and Proteasomal Pathways in Atrophying
711 Muscle Cells. *Cell Metabolism* 6: 472–483
712 Zhao S, Zhang J, Hou X, Zan L, Wang N, Tang Z & Li K (2012) OLFML3 expression is decreased during prenatal
713 muscle development and regulated by microRNA-155 in pigs. *Int J Biol Sci* 8: 459–469
714 Zhu J, Shi X, Lu H, Xia B, Li Y, Li X, Zhang Q & Yang G (2016) RNA-seq transcriptome analysis of extensor digi-
715 torum longus and soleus muscles in large white pigs. *Mol Genet Genomics* 291: 687–701
716

